

Microwave plasma torches used for hydrogen production

F M Dias, N Bundaleska, J Henriques, E Tatarova, and C M Ferreira

Instituto de Plasmas e Fusão Nuclear, Instituto Superior Técnico, 1049-001 Lisboa,
Portugal

E-mail: francisco.dias@ist.utl.pt

Abstract. A microwave plasma torch operating at 2.45 GHz and atmospheric pressure has been used as a medium and a tool for decomposition of alcohol in order to produce molecular hydrogen. Plasma in a gas mixture of argon and ethanol/methanol, with or without water, has been created using a waveguide surfatron launcher and a microwave generator delivering a power in the range 0.2–2.0 kW. Mass, Fourier Transform Infrared, and optical emission spectrometry have been applied as diagnostic tools. The decomposition yield of methanol was nearly 100 % with H₂, CO, CO₂, H₂O, and solid carbon as the main reaction products. The influence of the fraction of Ar flow through the liquid ethanol/methanol on H₂, CO, and CO₂ partial pressures has been investigated, as well as the dependence of the produced H₂ flow on the total flow and power. The optical emission spectrum in the range 250–700 nm has also been detected. There is a decrease of the OH(A-X) band intensity with the increase of methanol in the mixture. The emission of carbon atoms in the near UV range (240–300 nm) exhibits a significant increase as the amount of alcohol in the mixture grows. The obtained results clearly show that this microwave plasma torch at atmospheric pressure provides an efficient plasma environment for hydrogen production.

1. Introduction

In the recent years, great attention has been paid to the new hydrogen based technologies. Hydrogen is considered as a reliable alternative energy source, which liberates a considerable quantity of ecologically pure energy per unit weight (120 kJ/g) without emitting greenhouse gases [1]. Moreover, hydrogen can be viewed as a renewable fuel and it can be easily converted into electricity by fuel cells. Therefore, investigation of new hydrogen sources is of the utmost importance. The idea to focus on alcohols, especially ethanol, is due to the fact that it is a renewable resource in contrast to CH₄, which is usually used for this purpose. Ethanol can be obtained from cellulosic materials, corn or sugar.

Presently, hydrogen is produced by fuel processing technologies converting different hydrocarbons into hydrogen rich stream. The main conventional techniques used to produce hydrogen from hydrocarbon fuels (steam reforming, partial oxidation, and autothermal reforming) have problems like catalyst poisoning, size and weight requirements, compactness, dynamic behaviour (sluggish response), and limitations on hydrogen production from heavy hydrocarbons [1–5]. Among the possible innovative options, plasma systems can provide original solutions to these drawbacks [4–17]. In the plasma, the overall reforming reactions are in fact the same as in conventional reforming, but the energy and the free radicals used for the reforming reaction are provided by the plasma itself. The plasma eliminates the need for a catalyst in the systems. It plays a catalytic role because highly active species such as electrons, ions and radicals may significantly enhance the reaction rate. Plasma



systems can be applied to various hydrocarbons including natural gas, gasoline, heavy oils, and bio fuels, as well as biomass. Moreover, the plasma high energy density leads to compactness of the system and fast response times can be achieved due to the electrical operation of the system. Generally, non-thermal plasmas due to their non-equilibrium properties have low power requirements and capacity to induce physical and chemical reactions in gases at relatively low temperature [8]. Different types of non-thermal plasmas have been used for reforming of hydrocarbons: the corona discharge [10]; the dielectric barrier discharge (DBD) [12, 14]; gliding arc technology. The comparison between different arc discharge-based systems shows that the gliding arc technology meets the best performances due to its relative set-up simplicity and high flexibility, which allows operation over a wide range of flow rates and the treatment of a large amount of chemical species [8]. Different DC and AC corona discharges operating at room temperature have been applied to decompose alcohols for hydrogen production [15–17].

In this context, microwave discharge based systems, which are electrodeless, have not yet been thoroughly investigated as plasma reformers. Some results obtained with microwave discharges at reduced pressure are presented in [18]. Microwave plasmas operating at atmospheric pressure have been the subject of increased attention during the last decade as well. It has been shown that these torches provide suitable conditions to dissociate molecules in the abatement systems, to burn out chemical and biological warfare agents, and to atomize materials [19–30]. One of the main merits of microwave plasma torches at atmospheric pressure is that they make it possible to inject large power densities into the plasma and thus achieve high densities of active species of interest. An essential advantage of microwave plasmas over other types of discharges, such as gliding arcs, corona and dielectric barrier discharges, is the absence of electrodes [1–3]. In this way, problems such as electrode erosion, discharge pollution, and additional energy consumption for cooling are avoided. Besides, working at atmospheric pressure would also make the industrial application less complicated. The capability of microwave plasmas generated by surface waves at atmospheric pressure to decompose various alcohols (methanol, ethanol, butanol, and propanol) and to produce hydrogen has been tested in [31]. In particular, surface wave driven discharges offer several advantages over other types of discharges: they can operate with high stability and reproducibility over a large range of operation conditions; they require lower power to achieve similar values of electron density (note that electrons are responsible for the creation of active species and for the first step in the decomposition processes); they produce large plasma volumes with different possible geometries providing high enough residence times. The present investigation aims at finding optimal conditions for the plasma decomposition process of alcohol, i.e., the highest H_2 yield, the appropriate gas flow, input power and reforming substance (methanol/ethanol with or without water). For this purpose, plasma in a gas mixture of argon and methanol/ethanol (CH_3OH , C_2H_5OH) has been created using a waveguide surfatron based set-up [32]. The influence of the Ar "bubbling" flow through the liquid methanol/ethanol on the H_2 , CO_2 , and CO partial fluxes has been investigated. The dependence of the produced H_2 flow on the total Ar flow and power delivered to the launcher have also been analyzed. In order to investigate the contribution of steam reforming reaction, water vapor has also been introduced into the mixture. Mass spectrometry has been used to detect molecular hydrogen produced by methanol/ethanol decomposition. Fourier Transform Infrared Spectroscopy has been applied to detect different species such as H_2O , CO_2 , and CO molecules, which are produced as a result of plasma driven decomposition processes and subsequent association processes. The optical emission spectrum in the range 250–700 nm was investigated to detect the presence of the species of interest in the discharge.

2. Experimental set-up

A microwave plasma torch operating at 2.45 GHz and atmospheric pressure has been used. Plasma in a gas mixture of argon and alcohol (methanol/ethanol), with or without water, has been created using a waveguide surfatron launcher [32] and a microwave generator delivering a power in the range 0.2–2.0 kW. The generator is connected to a waveguide (WR-340) system, which includes an isolator,

directional couplers, and a 3-stub tuner. The above system is terminated by a movable short-circuit, which allows the maximization of the electric field at the launcher position. The discharge takes place in a quartz tube (1.5 cm inner and 1.8 cm outer diameters, respectively). The quartz tube is inserted vertically and perpendicularly to the waveguide wider wall. The total gas flow used in the experiments ranges from 500 to 4000 sccm. The argon gas used has a purity of 99.999 %. Alcohol (methanol/ethanol) is introduced into the discharge by bubbling Ar through the alcohol filled tank at room temperature as shown in the figure 1. The bubbling method allows one not to use any additional energy source in the process. The total flow Q_t consists of two parts. One part goes through the tank containing the alcohol to drag the molecules (bubbling). The resulting mixture (Ar + alcohol) flow Q_A is combined with the second part of pure Ar flow Q_{Ar} and the total flow $Q_t = Q_A + Q_{Ar}$ is then introduced into the quartz tube, where the discharge takes place. When water vapor is additionally introduced into the plasma, the pure Ar flow is divided in two different fractional “bubbling” flows. The first one is formed by “bubbling” of Ar through the alcohol tank, Q_A , and the second one is formed by “bubbling” of Ar through a water tank, Q_W . Then, the two fractional flows are combined and the total gas flow $Q_t = Q_A + Q_W$ is introduced into the discharge. The water in the tank was heated up to 70 °C.

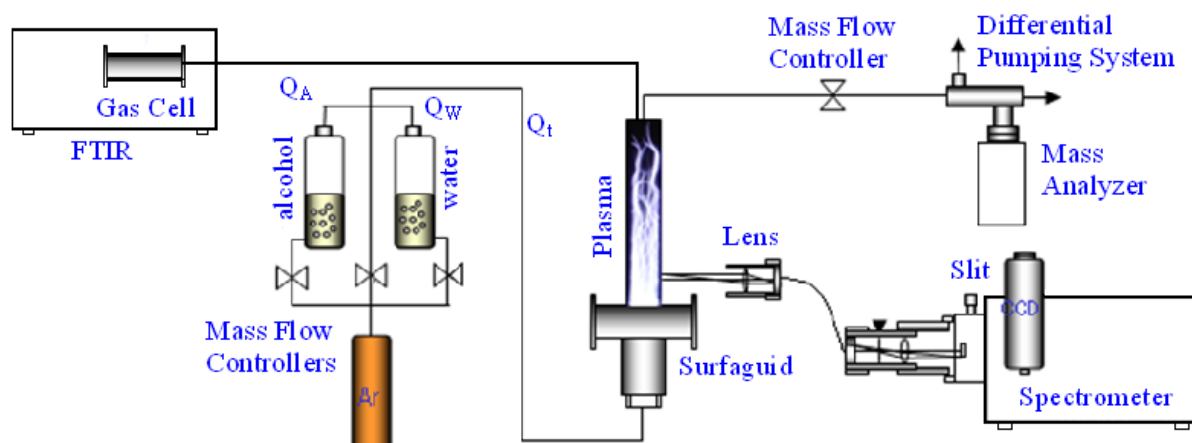


Figure 1. Experimental set-up

Three types of diagnostics have been carried out. Mass Spectrometry and Fourier Transform Infrared Spectroscopy (FTIR) have been used to analyze the exhaust gas stream fluxes. Gas sampled portions of the output gas stream from the plasma reactor were directed to the mass analyzer (Stanford Research System RGA 200) and to the FTIR spectrometer. The absorption spectra of H_2O , CO , CO_2 , and C_2H_5OH (ethanol) species were detected by a FTIR Termo Nicolet 5700 spectrometer in the wave number range of 1000–4000 cm^{-1} . At the same time, light emitted by the plasma radiative species was collected perpendicularly to the discharge tube by an optical fibre and directed to the entrance slit of a Jobin-Yvon Spex 1250 spectrometer equipped with a liquid–nitrogen cooled CCD camera. The plasma emission in the 250–850 nm range has been investigated.

3. Experimental results

In order to demonstrate the feasibility and effectiveness of the microwave plasma decomposition processes of methanol and ethanol, the hydrogen yield dependence on the fluxes and the microwave input power has been investigated both in Ar and Ar + water environments. Separate experiments have been performed for methanol and ethanol.

3.1. Decomposition of methanol

3.1.1. Influence of total flow rates and input power. The influence of the Ar “bubbling” flow Q_A , total flow Q_t , and microwave power delivered to the launcher on the molecular hydrogen production have been investigated. The species in the exhaust gas stream have been detected in order to investigate the effectiveness of the argon microwave plasma to break down the bonds of methanol molecules and release hydrogen molecules. There is a clear jump in H_2 partial pressure, as measured with the mass analyzer, when the microwave plasma is turned on, which is a clear evidence of H_2 production from methanol decomposition by the plasma. The time evolution of the H_2 partial pressure detected by the mass analyzer is presented in figure 2. The H_2 partial pressure increases with the Ar “bubbling” flow. The relative fractions of Q_A in the total flow Q_t were 3, 6 and 9 % in the above case. The investigation shows that the variation of Q_A is linearly correlated with the actual methanol flux (see figure 3). The CO partial pressure also shows linear dependence on Q_A . This is expected since H_2 and CO are the methanol dissociation products according to the reaction $CH_3OH \rightarrow 2H_2 + CO$ (R1). Other species detected by the mass analyzer (Ar, N_2 , H_2O) do not show changes when the plasma is turned on or turned off, which indicates that they are not related to processes in the plasma. Also, a small black deposit appears on the discharge wall when methanol is introduced in the Ar plasma environment.

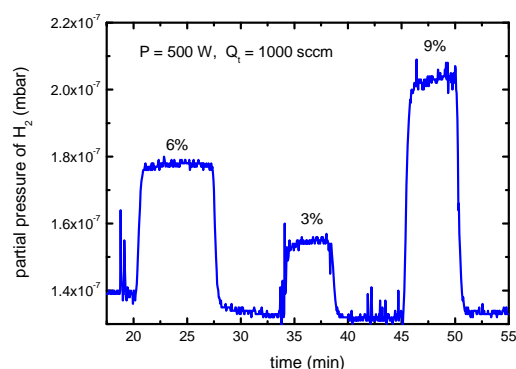


Figure 2. Time evolution of H_2 partial pressures during the plasma decomposition of methanol.

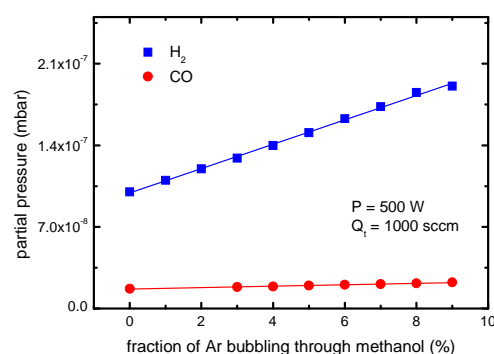


Figure 3. Dependence of the H_2 and CO partial pressures on the fraction of Ar bubbling through methanol.

The molecular hydrogen production dependence on the pure methanol flow for different total flows is shown in figure 4. The solid line shown on this figure represents the theoretical dependence according to the dissociation reaction (R1). As seen, for a total flux Q_t in the range 500–2000 sccm the produced hydrogen partial flow agrees with the predictions from (R1). This means that every CH_3OH molecule yields two H_2 molecules as a result of the plasma stimulated dissociation process (nearly 100 % efficiency of the process).

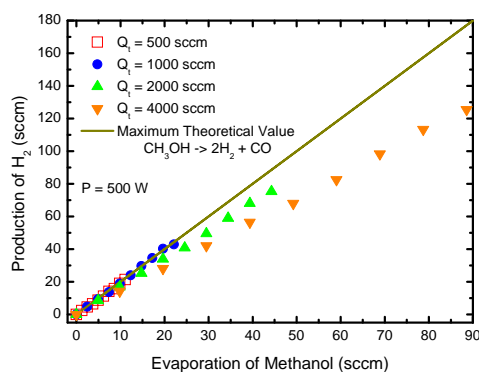


Figure 4. Hydrogen flow vs. pure methanol flow.

The microwave input power is also an important parameter in the plasma decomposition process. The microwave power absorbed per unit volume is linearly correlated with the electron number density. The electrons are responsible for the first step of the decomposition processes since they produce reactive species in the discharge via collisions with the gas atoms and molecules. The dependence of the hydrogen yield on the total microwave power delivered to the launcher in

the range 100–700 W is shown in figure 5. Here, the total flow Q_t and the fractional Ar “bubbling” Q_A flow are kept constant. The observed increase in hydrogen yield with the input power can be explained by the fact that more active species are generated at higher microwave power. However, some saturation in hydrogen production is observed for microwave powers greater than 400 W, which corresponds to a power density of about 10 W/cm^3 . This suggests that increasing power density above this value induces intensive chemistry involving dissociation of hydrogen molecules followed by association processes of highly reactive H atoms with other radicals to form hydrogen containing species.

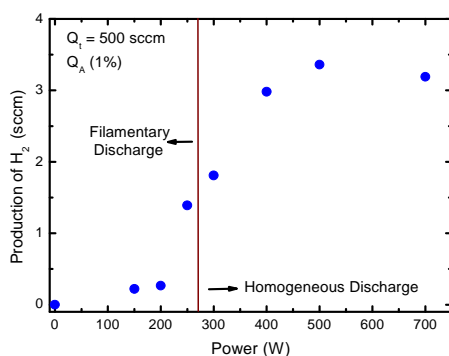


Figure 5. Dependence of H_2 flow on power

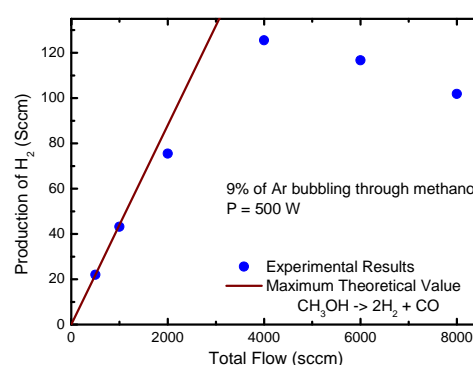


Figure 6. Dependence of H_2 flow on total flow

The influence of the total flow on the H_2 production is presented in figure 6. The fractional Ar “bubbling” Q_A flow is kept constant. As seen, for small total flow the H_2 production reaches the maximum theoretical value, i.e., the introduced methanol is all reformed. As the total flow increases, strong deviations from the maximum theoretical value and even a decrease in H_2 production above 4000 sccm are observed. This can be explained by the decrease of the amount of methanol in the mixture. Moreover, the residence time also decreases at higher gas velocities.

3.1.2. Effect of additional water vapor flow. The effect of a small addition of water vapor on the hydrogen and the carbon oxide/dioxide yields has also been investigated (figure 7). To this end, Ar “bubbling” flow through the water tank, Q_W , was combined with the Ar–methanol flow Q_A .

The water in the tank has been heated to about 70°C for this purpose. The corresponding chemical

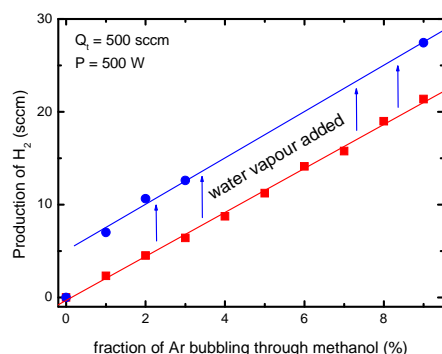


Figure 7. Produced H_2 flow vs. Ar “bubbling” Q_A flow through methanol

reaction is $\text{CH}_3\text{OH} + \text{H}_2\text{O} \rightarrow 3\text{H}_2 + \text{CO}_2$ (R2), and an increase in the H_2 and CO_2 yields is observed. It should be noted that the methanol decomposition reaction (R1) is followed by the so called water–gas shift reaction $\text{CO} + \text{H}_2\text{O} \rightarrow \text{H}_2 + \text{CO}_2$ (R3). The relative contribution of the latter reaction will depend on the quantity of introduced water: if there is enough water, CO should not be present at all. For very small methanol amounts, we observe in figure 7 a changing slope of H_2 production as water is added. The reason is that 3 hydrogen molecules per single methanol molecule are formed instead of 2. So, if the water quantity is larger or equal to that of methanol we can expect a 3:2 increase in H_2 production.

3.2. Decomposition of ethanol

3.2.1. Influence of total flow rates. An ethanol solution 96 % ethanol + water has been introduced in the Ar plasma environment by the “bubbling” method described above. Figures 8(a, b) show two FTIR spectra in the 1000–4000 cm^{-1} wave number range as obtained before and after the microwave plasma torch is applied, respectively, for 500 W of applied power, 500 sccm total Ar flow, and two different fractional Ar “bubbling” flows. The spectral lines at wave numbers around 3000 and 1000–1500 cm^{-1} are a signature of the ethanol presence in the exhaust stream before the plasma is turned on. Obviously, ethanol molecules are very efficiently decomposed in the Ar plasma environment and CO_2 and H_2O are observed as the by-products.

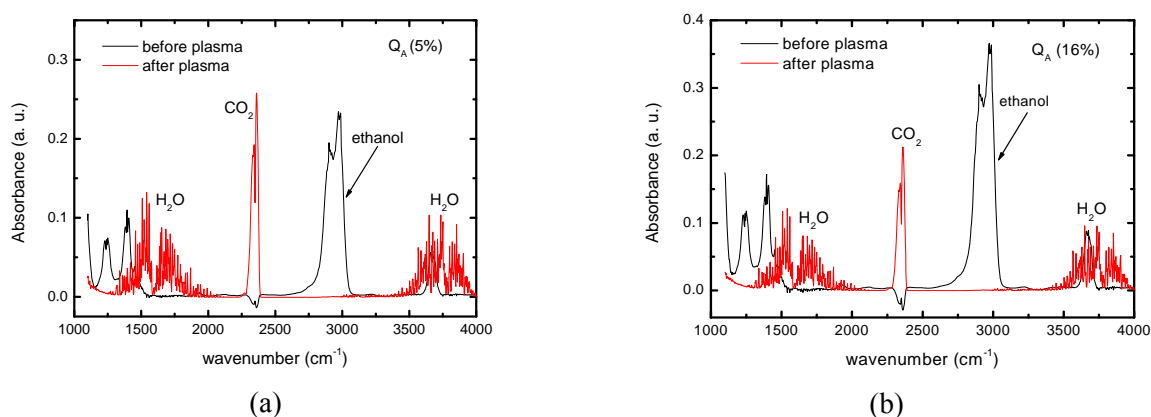


Figure 8. Infrared absorption spectra of Ar + ethanol mixture before and after plasma processing for two different fractional Ar “bubbling” flows Q_A (a) 5 and (b) 16 %. Total flow $Q_t = 500$ sccm.

Ethanol dissociates through the reaction $\text{C}_2\text{H}_5\text{OH} \rightarrow \text{CO} + 3\text{H}_2 + \text{C}$ (R4). The presence of CO_2 and water in the exhaust stream can be explained by the conversion of part of CO into CO_2 as a result of the water gas shift reaction (R3). Moreover, the presence of a small quantity of H_2O can initiate the steam reforming reaction $\text{C}_2\text{H}_5\text{OH} + \text{H}_2\text{O} \rightarrow 2\text{CO} + 4\text{H}_2$ (R5).

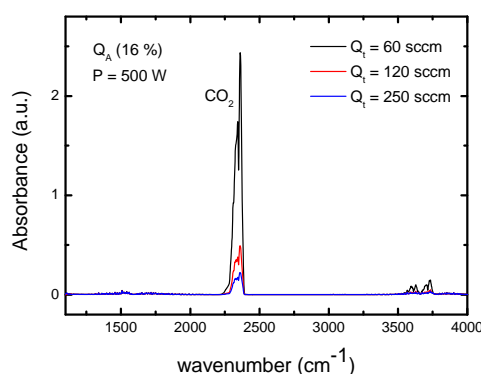


Figure 9. Infrared absorption spectra of Ar + ethanol mixture for different Q_t and constant Q_A .

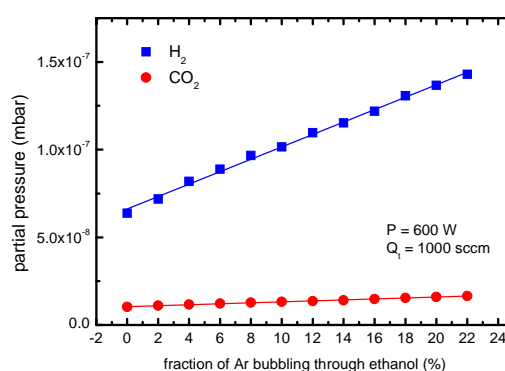


Figure 10. Dependence of H_2 and CO_2 partial pressures on the fraction of Ar bubbling through ethanol.

Indeed, the ethanol solution contains about 4 % of water, therefore steam reforming and water gas shift reactions do occur. The CO_2 absorption clearly decreases when the total Q_t flow increases at

constant ethanol percentage in the mixture (figure 9). It should be noted that Q_A or the ethanol percentage is kept constant. Thus, the relative amount of ethanol in the mixture decreases as the total gas flow increases, consequently the amount of CO_2 decreases. As in the methanol case, a black deposit on the quartz wall is formed due to the introduction of ethanol into the plasma. This indicates that some recombination reactions, such as $\text{C} + \text{C} (+ \text{wall}) \rightarrow \text{C}_2 (+ \text{wall})$, leading to C_2 formation are in play. Furthermore, association reactions such as $\text{C}_2 + \text{C}_2 (\text{wall}) \rightarrow \text{graphite}$ produce solid carbon (graphite) on the tube wall, as observed in the experiment. The dynamic behavior of the plasma decomposition system exhibits jumps in the H_2 partial pressure when the fractional Ar “bubbling” flow Q_A (i.e., the ethanol amount) increases (not shown here). The dependence of the H_2 and CO_2 partial pressures on the fraction of Ar bubbling through ethanol is presented in figure 10. As seen, the dependence is linear and the CO_2 partial pressure is nearly one order of magnitude smaller than that of molecular hydrogen.

3.2.2. Effect of additional water vapor. In order to investigate the influence of the steam reforming reaction, an additional quantity of water vapor was introduced by “bubbling” of Ar through the water tank as done before. The influence of the introduced amount of “pure” ethanol or ethanol + water into the plasma on the H_2 production is shown in figure 11. Three different values of the fractional Ar “bubbling” flow, Q_A , passing through the ethanol tank have been used, i.e., 5, 10 and 15 % (Q_W varies from 95 to 85 % of the total flux). In fact, the H_2 yields nearly double when water vapor is added.

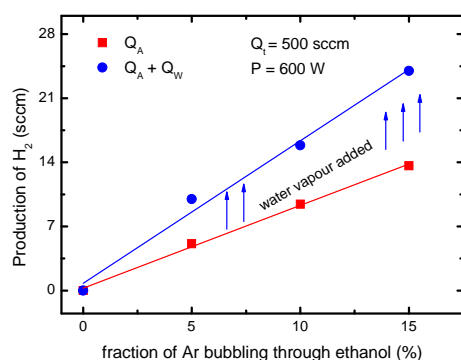


Figure 11. Produced H_2 flow vs. Ar “bubbling” Q_A flow through ethanol

Furthermore, no carbon black deposition was observed in this case, which seems to confirm that the steam reforming reaction is the dominant process of H_2 production here.

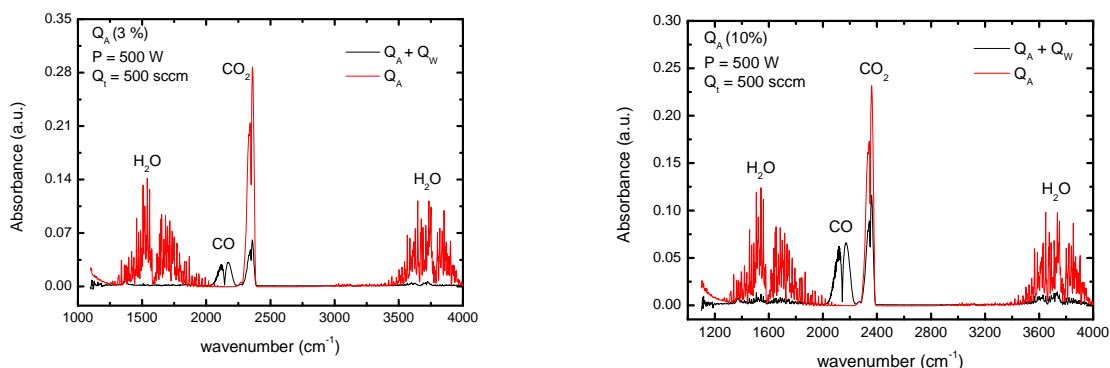


Figure 12(a, b). Infrared absorption spectra of Ar–ethanol–water vapor plasma for different fractional Ar “bubbling” flows Q_A .

4. Characterization of argon – alcohol – water plasma torch

The presence of alcohols and water vapor in the argon plasma torch change significantly the plasma characteristics. Optical emission spectroscopy has been applied to measure the gas temperature and the electron density as key plasma parameters. Usually, the rotational temperature of the OH radical is determined as a measure of the gas temperature. Here, the emission spectrum of the OH($A^2\Sigma^+, v=0 - X^2\Pi_i, v'=0$) (Q_1 branch) band in the range 306–315 nm was detected. The measured spectrum is shown in figures 13, 14. The rotational temperature has been determined by using the classical Boltzmann plot method. Assuming equilibrium, the intensity of the emission lines (I_R) of a rotational band can be expressed as [29]:

$$I_R = aA_jH \frac{c}{\lambda} \exp\left[\frac{-E_j hc}{kT_R}\right] \quad (1)$$

where a is a constant, A_j is the transition probability of rotational level j , h is the Planck's constant, c is the speed of light in vacuum, λ is the wavelength of the line, k is the Boltzmann's constant, T_R is the rotational temperature, and E_j is the energy of the emitting state. Using (1), the rotational temperature can readily be calculated from the slope of the Boltzmann plot $\log(I_R\lambda/A_j)$ vs. E_j .

The results were obtained in Ar–methanol and Ar–methanol–water vapor plasmas at constant total flow of 500 sccm and constant microwave power delivered to the launcher. The estimated gas temperature is typically around 3000 K when Q_A changes from 1 to 10 %. The presence of water in the plasma increases the gas temperature to about 3500–4000 K. The influence of the total flow Q_t on the gas temperature has also been investigated. The increase of Q_t from 500 to 4000 sccm contributes to an increase in gas temperature of about 15 %.

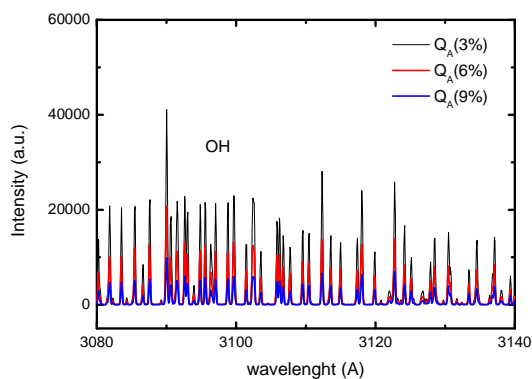


Figure 13. Intensity of OH(A-X) band emitted from Ar–methanol plasma at different Q_A .

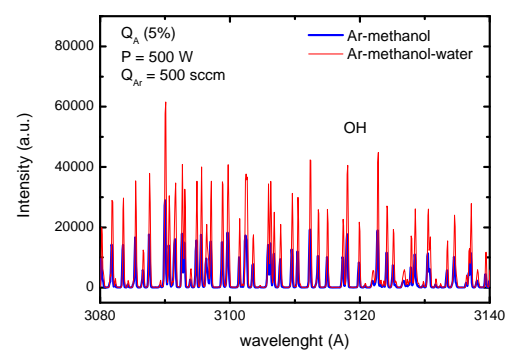


Figure 14. Intensity of OH (A-X) band emitted from Ar–methanol and Ar–methanol–water plasma

Figure 13 shows the spectrum of the OH(A-X) band emitted by the Ar–methanol plasma. As seen, there is a decrease in the OH(A-X) band intensity with the increase of methanol in the mixture. This suggests that the OH molecule dissociates with the increase of methanol. Adding water vapour increases the intensity of OH as expected (figure 14).

The electron density has been determined using the well known Stark broadening method. Since H_β was not detected in the present experiments, the H_α line has been used for this purpose. The measured line profiles have been well fitted by a Voigt function. Estimations show that resonance and natural broadening are negligible under the present conditions. A deconvolution procedure has been used to determine the full width at half-maximum of the Gaussian ($\Delta\lambda_G$) and Lorentzian ($\Delta\lambda_L$) components.

Stark and van der Waals broadening convolute to give a Lorentzian component. The measured gas temperature has been used to estimate van der Waals broadening ($\sim 0.116 \text{ \AA}$) and the latter was deconvoluted from the Lorentzian full width at half maximum to estimate the pure Stark broadening. Assuming that Ar atoms are the main perturbers, the expression for van der Waals broadening of the H_α line given in [30] has been used. The electron density has been calculated by fitting the widths listed by Gigos *et al* [34] for a reduced mass of 0.976, which corresponds to the present emitter – perturber conditions, i.e., the pair hydrogen–argon.

The values of electron density so determined at 2 cm from the launcher vary in the range $3.3 \times 10^{13} - 5.4 \times 10^{14} \text{ cm}^{-3}$, for a total flux varying from 500 to 2000 sccm, an Ar “bubbling” flux through alcohol kept constant at 4 %, and 500 W microwave power delivered to the launcher. It should be noted that the densities determined in this way correspond to radially averaged values.

5. Conclusions

A microwave plasma torch operating at 2.45 GHz and atmospheric pressure conditions has been used to create a plasma environment to decompose alcohols. Methanol/ethanol and water vapor have been introduced into the discharge by bubbling of Ar through the alcohol and water. Mass spectroscopy and Fourier Transform Infrared Spectroscopy have been applied to detect the molecular hydrogen produced by methanol/ethanol decomposition and H_2O , CO_2 and CO molecules in the exhaust gas stream.

The H_2 partial pressure increases when the Ar “bubbling” flow through methanol increases up to 10%, i.e., with the increase of the methanol amount. The highest H_2 yield in the case of methanol was obtained for relatively low argon flows (Q_t up to 2000 sccm). In fact, nearly 100 % decomposition of methanol was achieved by the Ar–methanol plasma torch operation. The optimal microwave power is about 400 W. Addition of water increases the H_2 production by about 50% but high H_2O flows influence the discharge stability.

The partial hydrogen flux in the exhaust stream of the Ar–ethanol plasma torch was observed to increase when the amount of ethanol (correlated with the Ar “bubbling” flow Q_A through the ethanol tank) increases. H_2O , CO, and CO_2 were detected as by-products of the plasma decomposition processes. Solid carbon as a black deposit on the tube walls was also observed. In Ar–ethanol–water vapor environment the measured H_2 partial pressure is nearly doubled in respect to the Ar–ethanol plasma. The steam reforming reaction $C_2H_5OH + H_2O \rightarrow 2CO + 4H_2$ is the most likely source of H_2 production in this case, which is confirmed by the fact that no solid carbon was observed. In addition, the main plasma characteristics, i.e., gas temperature and electron density, were experimentally determined for the Ar–methanol and Ar–methanol–water vapor plasmas. Gas temperatures around 3000 K and 3500 K – 4000 K were obtained for Ar–methanol and Ar–methanol–water vapor plasmas, respectively. The values of electron density vary in the range $3.3 \times 10^{13} - 5.4 \times 10^{14} \text{ cm}^{-3}$, for a total flux varying from 500 to 2000 sccm.

This work clearly shows that the present microwave plasma torch at atmospheric pressure can be very efficient for H_2 production from methanol/ethanol.

Acknowledgement

This work was supported by the Portuguese *Fundação para a Ciência e a Tecnologia* (FCT), under the research contract PTDC/FIS/108411/2008.

References

- [1] Holladay J D, Hu J, King D L and Wang Y 2009 *Cat. Today* **139** 244–60
- [2] Petitpas G, Rollier J-D, Darmon A, Gonzalez-Aguilar J, Metkemeijer R and Fulcheri L 2007 *Int. J. Hydrogen Energy* **32** 2848–67
- [3] Biniwale R B, Mizuno A and Ichikawa M 2004 *Appl. Catalysis A: General* **276** 169–77
- [4] Sekiguchi H and Mori Y 2003 *Thin Solid Films*, Elsevier, Jeju Island, South Korea 44–8

- [5] Bromberg L, Cohn D R, Rabinovich A and Alexeev N 1999 *Int. J. Hydrogen Energy* **24** 1131–7
- [6] O'Brien C J, Hochgreb S, Rabinovich A, Bromberg L and Cohn D R 1996 *Proceedings of the Intersociety Energy Conversion Engineering Conference, Hydrogen Production via Plasma Reformers* (IEEE, Piscataway, NJ, Washington DC, USA) 1747–52
- [7] Czernichowski A, Czernichowski P and Wesolowska K, Fuel 2004 *Cell Science, Engineering and Technology* (American Society of Mechanical Engineers, NY, USA) 669–76
- [8] Paulmier T and Fulcheri L 2005 *J. Chem. Eng.* **106** 59–71
- [9] Hammer T, Kappes T and Baldauf M 2004 *Cat. Today* **89** 5–14
- [10] Muta-Yardimci O, Saveliev A V, Fridman A A and Kennedy L A 1998 *Int. J. Hydrogen Energy* **23** 1109–11
- [11] Matsui Y, Kawakami S, Takashima K, Katsura S and Mizuno A 2005 *Energy and Fuels* **19** 1561–5
- [12] Jiang T, Li Y, Liu C-J, Xu G-H, Eliasson B and Xue B 2002 *Cat. Today* (Elsevier Science B.V., Washington DC) 229–35
- [13] Sobacchi M G, Saveliev A V, Fridman A A, Kennedy L A, Ahmed S and Krause T 2002 *Int. J. Hydrogen Energy* **27** 635–42
- [14] Sarmiento B, Javier Brey J, Viera I G, Gonzalez-Elipse A R, Cotrino J, Rico V J 2007 *J. Power Sources* **169** 140–3
- [15] Aubry O, Met C, Khacef A and Cormier J M 2005 *J. Chem. Eng.* **106** 241–7
- [16] Sekine Y, Urasaki K, Kado S, Matsukata M and Kikuchi E 2004 *Energy&Fuels* **18** 455–9
- [17] Sekine Y, Matsukata M, Kikuchi E, Kado S and Haga F 2004 (Prepr. Pap. Am. Chem. Soc.) *Div. Fuel Chem.* **49**(2) 914–5
- [18] Yanguas-Gil A, Hueso J L, Cotrino J, Caballero A and Gonzalez-Elipse A R 2004 *Appl. Phys. Lett.* **85**(18) 4004–6
- [19] Dubois D, Merbahi N, Eichwald O, Yosfi M and Benhenni M 2007 *J. Appl. Phys.* **101** 053304
- [20] Xinpei Lu and Laroussi Mounir 2005 *J. Appl. Phys.* **98** 023301
- [21] Ono Ryo and Tetsuji Oda 2005 *J. Appl. Phys.* **97**: 013302
- [22] Chen C K and Phillips J 2002 *J. Phys. D: Appl. Phys.* **35** 998–1009
- [23] Santiago I and Calzada M D 2007 *Appl. Spectroscopy* **61** 725
- [24] Ricard A, Jaoul C, Gaboriau F, Gherardi N and Villegier S 2004 *Surface&Coating Technology* **287** 188–9
- [25] Dato A, Radmilovic V, Lee Z, Phillips J and Frenklach M 2008 *Nano Letters* **8** 2010
- [26] Weigle J C, Luhrs C C, Chen C K, Perry W L, Mang J T, Lopez G P and Phillips J 2004 *J. Phys. Chem.* **108** 18601
- [27] Gleiman S, Chen C K, Datye A and Phillips J 2002 *J. Mat. Sci.* **37** 3429
- [28] Mills R, Ray P, Mayo R, Nansteel M, Dhandapanian B and Phillips J 2005 *J. Plasma Phys.* **71** 877
- [29] Phillips J and Chen C K 2008 *Int. J. Hydrogen Energy* **33** 7185
- [30] Oliveira C, Souza Corrêa J A, Gomes M P, Sismanoglu B N and Amorim J 2008 *J. Appl. Phys.* **93** 041503
- [31] Jimenez M, Yubero C and Calzada M D 2008 *J. Phys. D: Appl. Phys.* **41** 175201
- [32] Moisan M and Zakrzewski Z 1991 *J. Phys. D: Appl. Phys.* **24** 1025
- [33] Timmermans E A H, Jonkers J, Rodero A, Quintero M C, Sola A, Gamero A, Schram D C and van der Mullen J A M 1999 *Spectrochim. Acta B* **54** 1085